A Re-examination of the Aqueous Stability of Atomic Layer Deposited (ALD) Amorphous Alumina (Al_2O_3) Thin Films and the Use of a Post-Deposition Air Plasma Anneal to Enhance Stability

Simon A. Willis, Emily K. McGuinness, Yi Li, Mark D. Losego[#]

School of Materials Science and Engineering, Georgia Institute of Technology, Atlanta, Georgia 30332

[#]Email: losego@gatech.edu

Abstract

Amorphous aluminum oxide (alumina) thin films are of interest as inert chemical barriers for various applications. However, the existing literature on the aqueous stability of atomic layer deposited (ALD) amorphous alumina thin films remains incomplete and in some cases inconsistent. Because these films have a metastable amorphous structure—which is likely partially hydrated in the as-deposited state—hydration and degradation behavior likely deviate from what is expected for the equilibrium, crystalline Al_2O_3 phase. Deposition conditions and the aqueous solution composition (ion content) appear to influence the reactivity and stability of amorphous ALD alumina films, but a full understanding of why these alumina films hydrate, solvate, and/or dissolve in near neutral pH = 7 conditions, for which crystalline Al_2O_3 is expected to be stable, remains unsolved. In this work, we conduct an extensive X-ray photoelectron spectroscopy investigation of the surface chemistry as a function of water immersion time to reveal the formation of oxyhydroxide (AlOOH) and hydroxide species ($Al(OH)_3$). We further show that brief post-deposition exposures of these ALD alumina films to an air plasma anneal can significantly enhance the film's stability in near-neutral pH aqueous conditions. The simplicity and effectiveness of this plasma treatment may provide a new alternative to thermal annealing and capping treatments typically used to promote aqueous stability in ALD metal oxide barrier layers.

1. Introduction

Atomic layer deposition (ALD) of aluminum oxide (or "alumina") thin films is of interest for barrier layers in flexible electronics,[1-3] corrosion protection,[4] engineered biological systems, [5] catalyst overcoatings,[6] packaging devices,[7] and even as tarnishing barriers to preserve historical silver artifacts.[8] ALD is a chemical vapor deposition process that sequentially delivers precursors to achieve self-limited surface reactions that enable conformal coatings with sub-nanometer thickness precision.[9-10] One of the most commonly studied ALD reactions and materials is amorphous alumina (with an intended stoichiometry of Al_2O_3) synthesized from the reaction of trimethylaluminum (TMA) with water (H_2O).[11] However, based on existing literature, the aqueous dissolution behavior of these ALD alumina films is somewhat unclear, apparently dependent on the conditions of synthesis and post synthesis treatments, and possibly dependent on the dissolution environment itself. The focus of this paper is to review these inconsistencies, examine the chemical structure and aqueous stability of these amorphous ALD alumina films at a commonly used, low process temperature (150 °C), and clarify the dissolution response of these amorphous ALD alumina films under a range of solution compositions. We also demonstrate a simple new post-deposition treatment, exposure to an oxidizing plasma, to provide additional aqueous stability to these amorphous ALD alumina films.

2. Background

Table 1 summarizes the existing literature studies ("Reports") on amorphous ALD alumina thin film degradation, with rows sorted primarily by the *response* column and secondarily by the *post-processing column* (both black colored). Many factors likely contribute to degradation behavior, including aqueous solution pH, aqueous solution resistivity (or ion concentration), and ALD process conditions. However, many of the experiments in Table 1 are not intended to be

primary studies on the degradation behavior of ALD alumina, and thus do not directly report all of these parameters. Additionally, in some studies, the reported stability of these amorphous alumina films is inferred from a device stability metric, such as the photoemission current from a photoelectrochemical cell (PEC) experiment, as opposed to direct characterization of the alumina film thickness or structure. For these reasons, the study by Correa *et al.*[12] in Table 1 is highlighted, (gray rows) as it involves a direct study of ALD alumina degradation using ellipsometry and atomic force microscopy (AFM). This study characterizes ALD alumina film degradation in 4 different solutions and includes details about the solution environment, such as pH and resistivity, that improve the reproducibility of characterizing the degradation of the alumina films. The results generated by Correa *et al.* are compared to experiments in similar degradation environments in an attempt to extract critical synthesis, experimental, and characterization parameters that define the true degradation behavior of amorphous ALD alumina thin films.

In both acidic (H_2SO_4, 1M, Report #9) and basic (KOH, 1M, Report #8) solutions, Correa *et al.* report dissolution of their 40 nm ALD alumina films in approximately 48 hours and 12 hours, respectively. This result is consistent with the Pourbaix diagram for bulk crystalline alumina dissolution, which predicts Al_2O_3 instability outside the pH range of 5.8-7.3.[13] However, Fan *et al.*[14] report acidic stability (H_2SO_4, pH = 1, Report #1), with PEC J-V curves indicating device stability for up to 100 hours in solution. These two results can perhaps be reconciled if the methods of experimentation and characterization are considered more closely. In experiment 1, Fan *et al.* postulate that the measured hydrophobicity of the photocathode in their PEC experiment contributes to dynamic electrolyte-electrode contact, leading to decreased interaction rates between the Al_2O_3 and the H_2SO_4 solution. Additionally, Fan *et al.* perform indirect J-V curve characterization of their Al_2O_3 barrier performance. Considering these two experimental details, it

is possible that their Al_2O_3 films experimentally dissolve, but not to the extent that the underlying photocathode performance is affected, resulting in little to no change in the measured J-V curves.

Table 1: *Survey of literature reports for degradation behavior of ALD alumina thin films*

Report Number	Deposition Conditions	Post-Processing	Solution	pH or Resistivity	Dissolution Temperature	Response	Characterization Technique	Film Thickness	Comments	Citation
#1	200 °C, TMA/H_2O	None	0.5 M K_2SO_4/ 0.5 M H_2SO_4	1 (H_2SO_4)	25 °C	Stable	PEC J-V Curve	4.5 nm	Stable for 100 hr	14
#2	150 °C, TMA/H_2O	None	1M KCl	Not specified	25 °C	Stable	Ellipsometry/AFM	40 nm	n/a	12
#3	150 °C, TMA/H_2O	3 hr anneal at 900 °C	DI Water	18 MΩ	25 °C	Stable	Ellipsometry/AFM	40 nm	n/a	12
#4	120 °C, TMA/H_2O	None	NaCl	6.5	25 °C	Stable	Polarizations	10, 30, and 100 nm	Increasing stability with film thickness	4
#5	150 °C, TMA/H_2O	None	DI Water	18 MΩ	25 °C	Hydration	Ellipsometry/AFM	40 nm	Hydration/thickness increase in 15 days	12
#6	150 °C, TMA/H_2O	3 hr anneal at 450 °C	DI Water	18 MΩ	25 °C	Hydration	Ellipsometry/AFM	40 nm	Hydration/thickness increase in 15 days	12
#7	100 °C, TMA/O_2 Plasma	None	DI Water	Not specified	25 °C	Dissolve	Photoluminescence	10 nm	Sensor failure in 10 days	15
#8	150 °C, TMA/H_2O	None	1M KOH	14	25 °C	Dissolve	Ellipsometry/AFM	40 nm	Full dissolution in 12 hours	12
#9	150 °C, TMA/H_2O	None	1M H_2SO_4	0	25 °C	Dissolve	Ellipsometry/AFM	40 nm	Full dissolution in 2 days	12
#10	175 °C, TMA/H_2O	None	Water Vapor (100% RH)	Not specified	25 °C	Dissolve	WVTR/HTO	26 nm	Dissolution in 120-180 hours	2
#11	100 °C, TMA/O_2 Plasma	None	Unspecified Water	Not specified	90 °C	Dissolve	FESEM/AFM/Conductance/WVTR	50 nm	Corrosion/dissolution in 30 minutes	1
#12	120 °C, TMA/H_2O	None	Chromatography Water	Not specified	90 °C	Dissolve	Ellipsometry/OM	20 nm	Corrosion/dissolution in 75 hours	16

More interesting is the consistent reports of degradation of amorphous ALD alumina films in near neutral pH conditions (pH near 7). Pourbaix diagrams predict aluminum metal to be stable in near neutral pH conditions, but the passivation layer formed to protect the metal may be either an oxide or an oxyhydroxide. With respect to the aqueous stability of alumina, Pourbaix's text describes several pathways for instability of γ-Al_2O_3 in boiling water but indicates low solubilities for α-Al_2O_3 polytypes in room temperature water. Pourbaix does indicate that the degradation of crystalline α-alumina depends on its "temperature of preparation" and how hydrated it is to start; fully dehydrated crystalline alumina should lose its hygroscopic nature and be stable in water.[13]

Thusly, Correa *et al.* (Report #5) report a measured increase in both ellipsometry-measured film thickness and AFM-measured film roughness of ALD-deposited alumina after approximately 10 days in 18 MOhm-cm resistivity deionized (DI) water at room temperature. Similarly, Bulusu *et al.*[15] (Report #7) report failure of a Ni sensor capped with a 10 nm ALD Al_2O_3 film after 10 days of immersion in deionized water at room temperature. In an unspecified water solution at 90° C, Kim *et al.*[1] (Report #11) directly measure surface roughening of their alumina films via FESEM and AFM measurements in as little as 30 minutes, corroborated by thickness increases and index of refraction decreases measured by ellipsometry. In chromatography water at 90° C, Abdugalatov *et al.*[16] (Report #12) measure dissolution of their alumina films via ellipsometry and optical microscopy in approximately 75 hours. The dissolution reported in Report #12 when compared to the presumable hydration in Reports #5, #7 can perhaps be attributed to the higher solution temperatures in Report #12, which should accommodate more dissolved species. Alternatively, Reports #5 and #7 use deionized water whereas Report #12 uses "chromatography water", and ions in this aqueous solution may be playing a role.

The above results can perhaps be understood by considering the expected physicochemical structure of the amorphous ALD alumina film. As prepared amorphous ALD alumina films are likely to be reasonably hydrated[17] (i.e., contain hydroxyl groups) and highly defective.[15,18] Existing hydroxyl groups or hydrated alumina regions can likely provide targets for reaction with water to form oxy-hydroxide compounds of the form $AlO_{(x)}OH_{(y)}$. These hydrated species are known to be removed at higher ALD deposition temperatures, with these films showing higher refractive index and density[19], although there is no clear evidence that changes in deposition temperature below 200 °C – the typical range for amorphous alumina ALD – have any significant effects on the dissolution response (Table 1). In an extreme case (Report #3), Correa *et al.* repeat their

experimental conditions for Report #5 but add a post-ALD thermal annealing treatment for 3 hours at 900°C. This annealing treatment is observed to crystallize the alumina film to a polycrystalline γ-Al_2O_3 phase, which presumably also has a very low concentration of hydroxyl groups. These crystalline γ-Al_2O_3 films were insoluble in room temperature DI water, perhaps consistent with the thermodynamic expectations for crystalline Al_2O_3 from the Pourbaix diagram.

In summary, differences observed among similar experiments in Table 1 can be attributed largely to **(1)** differences in testing and characterization conditions (Reports #1, 8, and 9), and **(2)** differences in the post-processed structure of the Al_2O_3 (Reports #3, 5, 6, 7, 11, and 12). In this paper we seek to better understand the chemical stability of amorphous ALD alumina films in a variety of aqueous solution conditions and provide better clarity for the physicochemical mechanisms driving the dissolution of these non-equilibrium amorphous films. We also examine the use of an air plasma anneal as a simple and conformal post-deposition treatment to enhance aqueous stability. Plasmas are known to alter the structure and crystallinity of nanoparticles[20-21] and induce densification in Al_2O_3 ceramic powders.[22] Here we show that simple room temperature air plasma treatments can also improve the aqueous stability of these amorphous ALD alumina films.

3. Experimental Methods

3.1 Atomic Layer Deposition of Alumina Thin Films: Alumina deposition was carried out in a custom-made 1.5-inch inner-diameter flow-tube ALD reactor with custom control software.[23] Nitrogen carrier gas (99.995% purity) was continuously flowed at 75 sccm and 1.2 Torr during the process. Films were grown on polished silicon substrates (WRS Materials, p-type/boron-doped)

using a trimethylaluminum (TMA, Strem, 99%, DANGER: Pyrophoric) and deionized (DI) water chemistry. Films were deposited for 400 cycles of TMA and H_2O at a temperature of 150 °C, giving a film thickness of about 44 nm. Prior to deposition, silicon wafers were plasma cleaned (HARRICK PLASMA CLEANER PDC-001-HP) for 5 minutes to remove organic surface contaminants and generate surface hydroxyls. After ALD deposition, but prior to dissolution testing, some films were left untreated by plasma (designated as "ALD-only") while others were exposed to an air plasma (designated as "plasma treated") for 5 minutes at 1.1 Torr of air at 30 W in the same Harrick plasma system (**Figure 1a, b**).

Dissolution testing (**Figure 1c**) was carried out in the dark in sealed 20 mL glass scintillation vials containing 10 mL of the aqueous test solution. Several neutral pH, deionized "types" of water were tested. These water "types" included deionized laboratory water of resistivity of 10 MOhm-cm (created with a Thermo Scientific B-Pure deionization unit), and Type I and Type II bottled deionized water purchased from Sigma-Aldrich. Type I water was measured to be 18 MOhm-cm resistivity, while Type II water was measured to be 1 MOhm-cm resistivity. Other aqueous solution of interest were also tested including a neutral (6.9 – 7.1 pH) phosphate buffer solution (PBS, VWR Materials) commonly used for biological specimens, a 0.5 M NaCl salt solution, a 0.25 M NaOH base solution (~13.4 pH), and a 0.5 M HCl acid solution (~.30 pH), all purchased from Sigma-Aldrich.

In order to minimize error from repeated measurements of the same alumina films and limit atmospheric exposure, each ellipsometry measurement contributing to a single time point was taken from a unique film. In other words, films were not re-immersed in solution after characterization via ellipsometry or XPS. When films were re-immersed in solution following characterization, reproducibility of some of the experiments was affected (Figure S1).

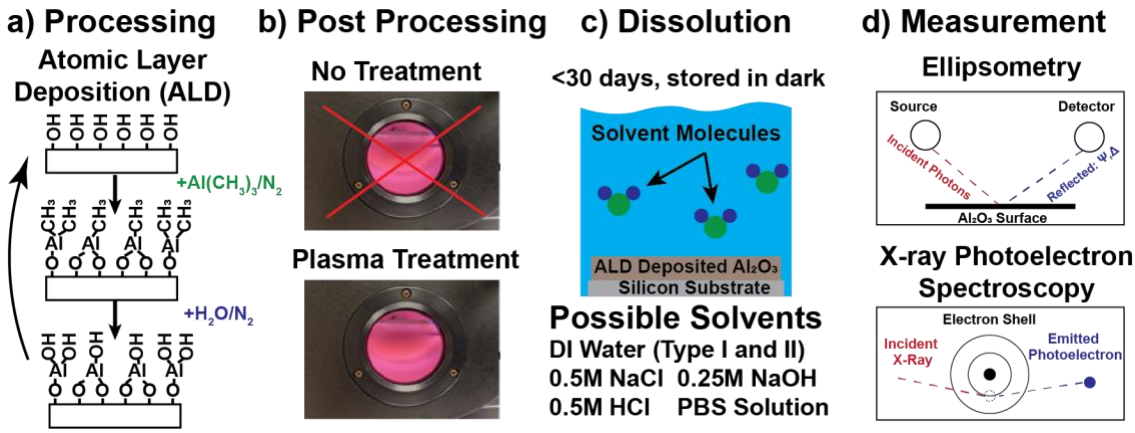

Figure 1. *Process flow diagram for alumina dissolution experiments. (a) Film are first deposited via ALD. (b) Films then either receive or do not receive a post-deposition plasma treatment. (c) Dissolution behavior is tested in the dark in various solution chemistries including Bottled DI water of types I and II, 0.5 M NaCl, 0.5 M HCl, 0.25 M NaOH, and pH 7 phosphate buffer solution (PBS). (d) Film dissolution is then investigated with spectroscopic ellipsometry and X-ray photoelectron spectroscopy (XPS).*

3.2 Thickness Measurements with Spectroscopic Ellipsometry: Film thickness was measured with a J.A. Woollam Alpha-SE ellipsometer at a 70° incident angle (**Figure 1d**). Measurements were fit using a Cauchy model for the film's optical constants using the J.A. Woollam CompleteEASE software. For more complex analysis of conditions deviating away from simple dissolution, a 5-layer graded Cauchy model was found to yield the lowest mean squared error (MSE) value. A comparison of ellipsometry models used and a detailed method of analysis is provided in Figure S2 of the SI. Each reported data point (e.g. each time point for each solvent) is an averaged thickness measurements of either 2 or 3 independent films each measured at 3 different locations.

3.3 X-Ray Photoelectron Spectroscopy: X-ray photoelectron spectroscopy (XPS) was used to evaluate the chemistry of thin films before and after immersion in aqueous solutions. XPS was conducted with a Thermo Scientific K-Alpha system using a monochromatic Al Kα X-ray source

(1486.6 eV) with a 60° incident angle and a 90° emission collection geometry. High-resolution scans were taken with a 0.10 eV step size. XPS curve fitting was conducted with Thermo Scientific Avantage Software. To ensure accuracy of measurements for the insulating surfaces, all spectra are charge referenced to C 1s = 284.8 eV. Deconvolution of the C1s spectra is carried out by fitting core-level peaks to several Gaussian peaks of similar FWHM ranges of 1.4-1.5 eV. O 1s deconvolution similarly fits to Gaussian peaks of FWHM ranges of 1.8-1.9 eV, while Al 2p deconvolution fits to Gaussian peaks of FWHM ranges of 1.5-1.6 eV. Once peak positions were identified for a given oxidation state, these energies were held constant for all fits by manually fitting peak energy positions to be consistent with the assigned energies.

4. Results and Discussion

4.1 Dissolution of ALD-only and Plasma Treated Alumina Thin Films in DI Water:

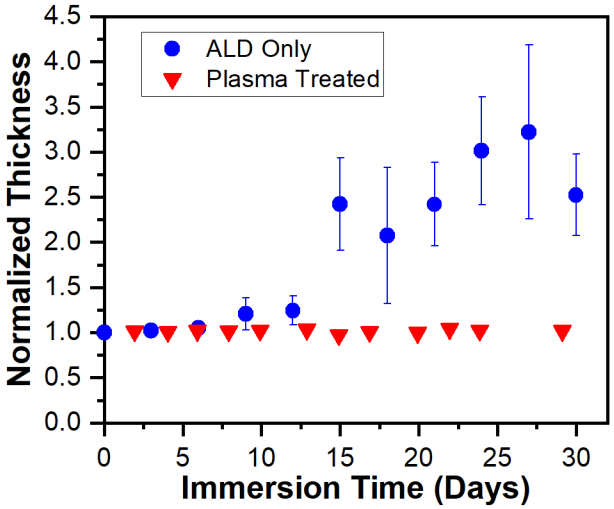

Figure 2: *Ellipsometry measured thickness of amorphous ALD alumina films upon immersion in 18 MOhm-cm Type I deionized water as a function of water immersion time. The normalized thickness is calculated by dividing the thickness by the film's initial thickness at 0 days (prior to immersion). Error bars represent standard errors for at least 3 films each measured at 3 separate locations (9 measurement points).*

Figure 2 illustrates a key result of this work: amorphous alumina ALD films degrade via hydration (get thicker) after about 7 days of immersion in near-neutral pH deionized water while post-deposition plasma annealed films exhibit good stability under the same aqueous conditions. In this figure the alumina films are immersed in 18 MOhm-cm Type I DI water for up to 30 days and film thickness is tracked with spectroscopic ellipsometry. The thickness ratio reported here is calculated by dividing each film thickness by the film's original thickness. After 7 days of immersion, the ALD-only alumina film begins to increase in thickness. This result is consistent with data reported by Correa *et al.*[12] This increase in film thickness is likely due to increased hydration of the alumina film (*vide infra)*. Correa *et al.* further correlated this change in thickness to morphological roughening of the film as imaged with AFM. The change in thickness reported here was fit to several ellipsometry models—including the simple isotropic Cauchy, the graded Cauchy, and a roughness Cauchy model—and all gave similarly trending results. Figure 2 shows the results of the graded Cauchy model, which is the best at minimizing the mean squared error of the measurements (see also Figure S2 for more modelled results). In contrast, the amorphous ALD alumina film exposed to a 5 min air plasma treatment showed no indication of change in film thickness nor refractive index, indicating stability in near-neutral pH conditions.

4.2 XPS Analysis of ALD-only and Plasma Treated Alumina Films before and after Water Immersion: To better understand the amorphous alumina's surface chemistry during water exposure, we performed detailed XPS analysis before water immersion and after 3 and 15 days of water immersion. In our analysis we examine both an ALD-only film and an alumina film exposed to an air plasma treatment. According to the ellipsometry data shown in **Figure** 2, 3 days is prior to significant hydration of the ALD-only alumina film and 15 days is near "complete" hydration.

A summary of XPS survey results for the O 1s and Al 2p peaks are given in Table S1. Figure 3 plots the O:Al ratio calculated from the O 1s and Al 2p peaks of these XPS spectra. The XPS data for the plasma treated condition at 9 days is removed due to poor data quality and noise in the Al 2p and O 1s spectral lines. We interpret these O:Al ratios as indicative of the extent of hydration of the oxide phase (hydrated phases have higher O:Al ratios). Initially, the ALD-only alumina film has an O:Al ratio of about 1.5, as expected for the Al_2O_3 sesquioxide. Interestingly, the surface chemistry of the plasma-treated alumina films is actually somewhat deficient in O compared to the sesquioxide phase, with an O:Al ratio of about 1.37. With water immersion, the O:Al ratio increases for both the ALD-only and plasma annealed alumina films. For ALD-only alumina films, the O:Al ratio approaches 2.5 after 15 days, while the air plasma treated film remains below 2.0, suggesting that the ALD-only film is significantly hydrated while the plasma treated film is not.

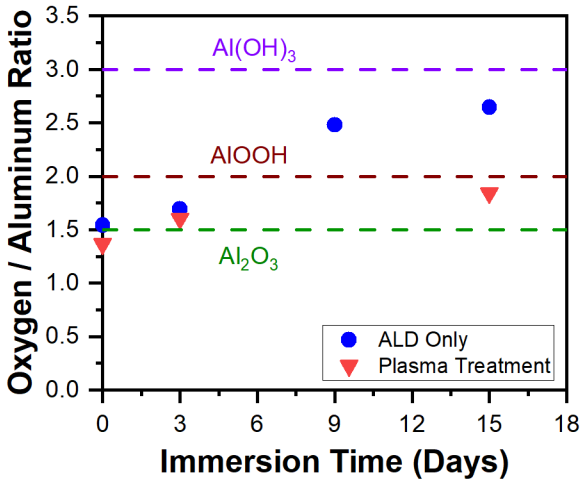

Figure 3: *Oxygen-to-aluminum elemental ratios calculated from XPS spectra using the Thermo Avantage software. Ratios for both the ALD-only alumina films (blue circles) and air plasma treated films (red triangles) are plotted as a function of water immersion time. The stoichiometric values for the sesquioxide Al_2O_3 (green dotted line), AlOOH (crimson dotted line) and $Al(OH)_3$ (purple dotted line) are also plotted for comparison.*

Hydroxylation of amorphous Al_2O_3 likely follows one of these three reaction pathways: (thermodynamic data taken from refs. 24 and 25)[24-25]

$Al_2O_3 + H_2O \rightarrow 2AlOOH$ ΔG_{rxn} = -62.268 kJ/mol at 25 °C **Reaction 1**

$AlOOH + H_2O \rightarrow Al(OH)_3$ ΔG_{rxn} = -2.206 kJ/mol at 25 °C **Reaction 2**

$Al_2O_3 + 3H_2O \rightarrow 2Al(OH)_3$ ΔG_{rxn} = -66.680 kJ/mol at 25 °C **Reaction 3**

Note that these free energy calculations use the free energy of formation for a configurationally frozen liquid alumina phase, which is used as a representation of the amorphous alumina. All three reactions are thermodynamically favorable when this representative amorphous Al_2O_3 is exposed to water at room temperature (i.e., negative free energies of reaction). Further, these thermodynamic calculations become less favorable for crystalline forms of alumina. For example, if Reaction 1 is re-written with the Gibbs energies of pure crystalline α-alumina (corundum) from reference 25, the overall free energy of reaction increases to -12.018 kJ/mol at 25 °C. This trend suggests that hydration is more favorable in amorphous alumina films than in crystalline alumina films, similar to what is implied in the Pourbaix text.[13]

Each of the possible hydrated products from reactions 1-3, AlOOH and $Al(OH)_3$, have higher O:Al ratios than Al_2O_3. AlOOH has an O:Al ratio of 2 while $Al(OH)_3$ has a ratio of 3. The observed XPS O:Al ratio of about 2.5 after 15 days of immersion suggests that the ALD-only alumina film forms a mixture of AlOOH oxyhydroxide and the $Al(OH)_3$ hydroxide with stoichiometric ratios similar to the thermodynamic alumina phases of boehmite and gibbsite, respectively. The plasma treated alumina ALD film's O:Al ratio remains near 1.8 even after 15 days of immersion, suggesting significantly less hydration, below even the amount for the oxyhydroxide.

High resolution XPS scans of the Al 2p (**Figure** 4) and O 1s (**Figure** 6) excitations provide further evidence for hydration of the ALD-only alumina films. First consider the Al 2p spectra in **Figure** 4. The existence and identity of one primary peak in the alumina system is well documented. In the literature, this peak is reported to be between 73.8 and 74.3 eV and is ascribed to O-**Al**-O bonding, irrespective of alumina phase or morphology.[26-33] A similar primary peak is observed in **Figure** 4 at 74.1 eV and is assigned to the amorphous sesquioxide phase. A second higher energy peak is often ascribed to the hydroxylated Al^{3+}. This peak is reported between 74.4 and 75 eV.[30, 34] This higher energy peak is also observed in this work at 74.7 eV, and is assigned to a boehmite-type structure with approximate stoichiometry of AlOOH. Additional reports exist for an even higher energy peak approaching binding energies of 76 eV.[31, 35-36] However, this peak is attributed to a number of different stoichiometries, including but not limited to AlOOH, $Al(OH)_3$, AlO_x, and Al_2O_3. A peak in this range of energies is observed in this work at 75.7 eV and is easily separated from lower energy states due to the strong shouldering effect observed on the higher energy side of the Al 2p spectral line (Figure 4e). Here, we assign this peak to the $Al(OH)_3$ stoichiometry, partially due to the previous thermodynamic analysis showing the favorability of formation of $Al(OH)_3$ in this system and the general trend that more -OH groups tend to increase the Al 2p binding energy. Additionally, the presence of this high energy peak is coincident with the increase of the oxygen/aluminum ratio to above 2.0, suggesting formation of a hydroxylated compound of higher oxygen content than AlOOH, such as $Al(OH)_3$. A final minor peak is observed at 72.8 eV. This peak is attributed to aluminum-carbon bonding from residual, unreacted trimethyl-aluminum precursor, the identity and presence of which is investigated in more detail in the C 1s spectral analysis (*vide infra*). However, we do note that this Al-C peak, while necessary for proper

deconvolution, is close to the noise level of the XPS scan, and thus serves only as a qualitative indicator of carbonaceous defects in the film.

Before immersion, the Al 2p spectrum for the ALD-only alumina film shows 79% emission from the Al_2O_3 oxide state, 17% emission from the AlOOH oxyhydroxide state, and 3% emission from the Al-C state, based upon relative peak areas (**Figure** 5). Interestingly, the plasma treated Al_2O_3 film has a similar Al 2p spectrum with 81% Al_2O_3 emission, although the quantity of AlOOH is somewhat reduced to 16%. After 3 days of water immersion, the Al 2p spectrum for the ALD-only alumina film shifts to higher binding energy, corresponding to an increase in AlOOH peak percentage to 50%. This result is interesting in that the ellipsometry results do not indicate any significant change in film thickness. These XPS results suggest that the hydration process is occurring sooner than can be detected with ellipsometry, or that the initial hydration reaction to form AlOOH does not involve significant restructuring of the film's morphology. After 9 days of immersion, the Al 2p peak for the ALD-only alumina film shifts to even higher binding energies with an AlOOH peak percentage of 64%, and upon deconvolution a new peak at 75.7 eV appears with a peak area percentage of 10%. Upon longer immersion of up to 15 days, the emission attributed to $Al(OH)_3$ continues to grow to an area percentage of 24%, while the peak attributed to AlOOH decreases to an area percentage of 41%. This decrease in the peak area of AlOOH suggests the AlOOH is being consumed in a hydration reaction to form $Al(OH)_3$ as per Reaction 2 above.

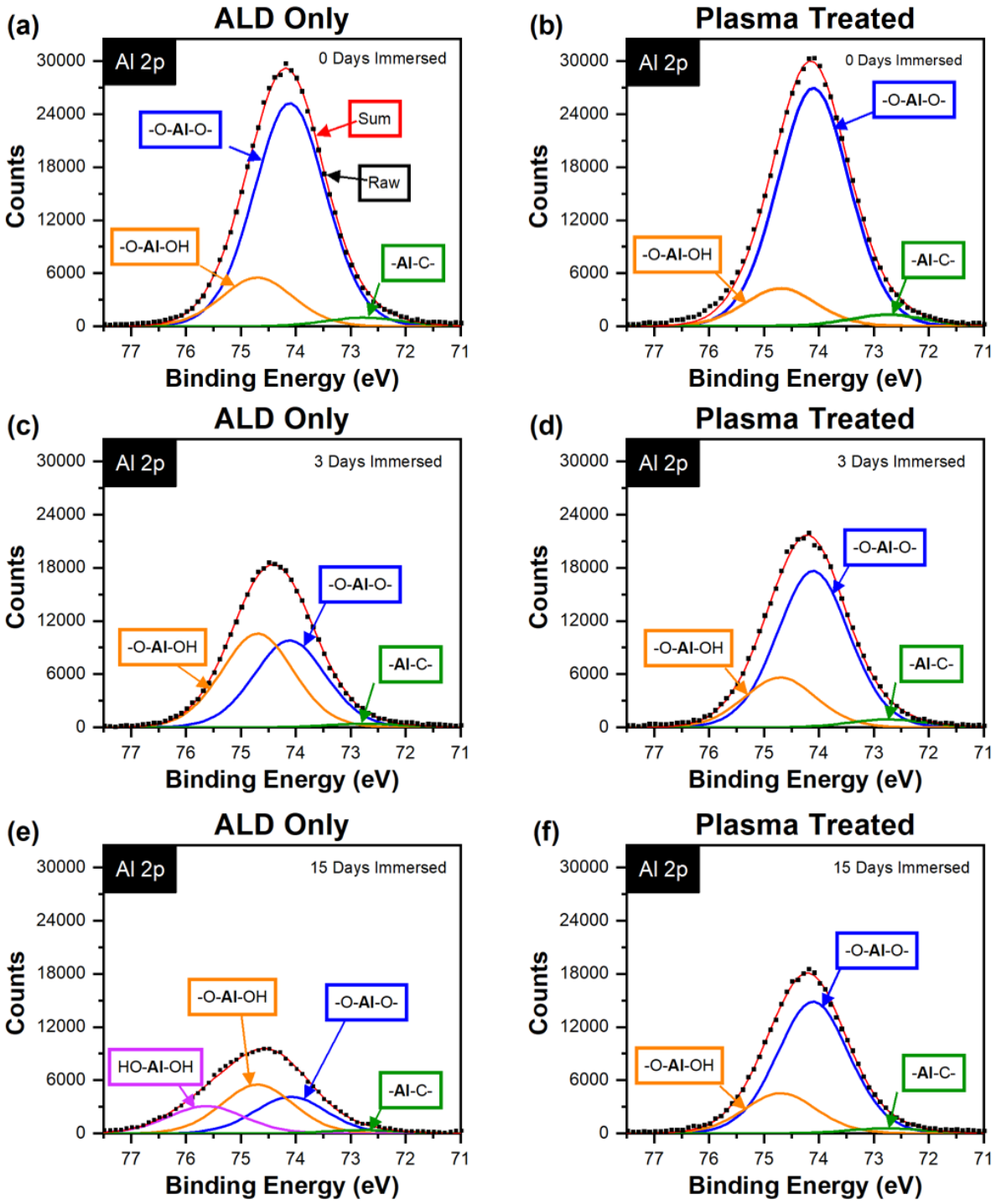

Figure 4: *Deconvoluted Al 2p XPS spectra for ALD-only and plasma treated alumina films before and after water immersion. (a) ALD-only and (b) plasma-treated alumina freshly prepared. (c) ALD-only and (d) plasma-treated alumina after 3 days of immersion in 18 MOhm-cm DI water. (e) ALD-only and (f) plasma-treated alumina after 15 days of submersion in 18 MOhm-cm DI water. Individual deconvoluted peaks are labelled and colored by their assigned approximate binding environment. The summation of these deconvoluted peaks is plotted as a*

solid red line which can be compared to the raw data (black squares) in each plot as a measure of goodness of fit.

We postulate that these $Al(OH)_3$ species are dissolving in the water and then redepositing to create the increase in film thickness observed with ellipsometry. The data plotted in Figure 5 suggests that the AlOOH is particularly susceptible to further hydration to the $Al(OH)_3$ state, although it is interesting to note that even after 15 days, a significant fraction of the XPS signal can still be attributed to the pure O-Al-O oxide structure (30% of the peak area).

In contrast, the air plasma annealed alumina film shows only a modest increase in Al-O-H content after 3 days of water immersion and virtually no change beyond 3 days (Figure 5b). As indicated in Figure 3, the hydroxide content remains below that expected for bulk AlOOH, suggesting that the hydroxides that are detected may only be surface hydroxide species and that the subsurface or bulk of the alumina is not becoming hydrated.

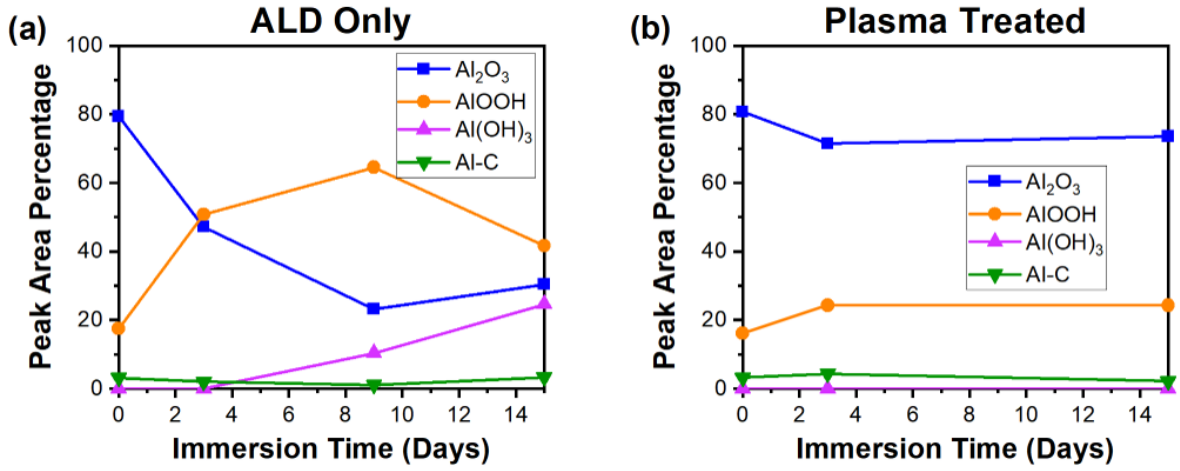

Figure 5: *Relative peak areas in the Al 2p XPS spectra as a function of water immersion time for both (a) ALD-only and (b) plasma treated alumina films in 18 MOhm-cm Type I DI water. Peak area percentages are calculated by dividing the peak area of the given peak by the combined area of all deconvoluted peaks for that Al 2p spectrum. Data sets are labeled with their inferred O:OH stoichiometries.*

The O 1s spectra in Figure 6 further confirm the interpretation of the results inferred from the Al 2p XPS data. The emission energies and chemical identities for O 1s peaks in the alumina system are well documented in the literature. The primary Al-**O**-Al bond associated with the stoichiometric sesquioxide is found at ~530.5-531.5 eV.[26-27, 30-31, 37] Here, we observed this peak at 531.0 eV. A peak associated with the Al-**O**-H bonds found in boehmite, pseudo-boehmite, and gibbsite is reported to occur at ~531.8-532.1 eV.[26, 30-31, 37] We also observe an emission at 532.0 eV. A third emission peak is observed at 533.1 eV and is ascribed to the presence of oxidized carbonaceous species (C-Ox), which are discussed in some detail below. Before immersion, the O 1s spectra for ALD-only alumina is composed of 67% Al-**O**-Al, 19% Al-**O**-H structure and about 6% C-Ox (**Figure** 7). The O 1s spectrum for plasma treated alumina is similar, with slightly reduced Al-**O**-H at 18% and slightly increased C-Ox at 9%. At 3 days immersion, the O 1s spectrum for the ALD-only alumina film increases in binding energy due to an increase in the area of the Al-**O**-H peak to 47% and a decrease in the area of the Al-**O**-Al peak to 40%. This binding energy shift is also accompanied by an increase in the C-Ox to 9%. After 9 days of immersion, the binding energy continues to increase as the Al-**O**-H peak area increases to 54%. After 15 days of immersion, the Al-**O**-H peak recedes slightly to 46%, while the C-Ox content continues to increase to 19%. By comparison, the C-Ox in the plasma treated films only changes slightly, from 9% at initial immersion to 10% at 15 days of immersion. The plasma treated films also increase in Al-**O**-H emission from 19% at immersion to 49% at 15 days. This suggests that the plasma treated films experience some chemical hydroxylation, like the ALD-only films, but the hydroxylation never proceeds to the extent necessary to significantly impact the film thickness as measured by ellipsometry. This observation could be consistent with the fact that the ALD-only films

experience a change in film thickness only after observation of the $Al(OH)_3$ peak at 9 days immersion, suggesting that formation of $Al(OH)_3$ is the predominant factor in film restructuring and detected increases in film thickness. Additionally, by looking at the C-Ox content of the two conditions, it is likely that the amount of C-Ox on the films corresponds to the amount of surface restructuring as a result of $Al(OH)_3$ formation. This implies the restructuring is increasing the surface area of the films, leading to an increase in adsorption sites and thus an increase in the area percentage of the C-Ox peak in the O 1s spectra.

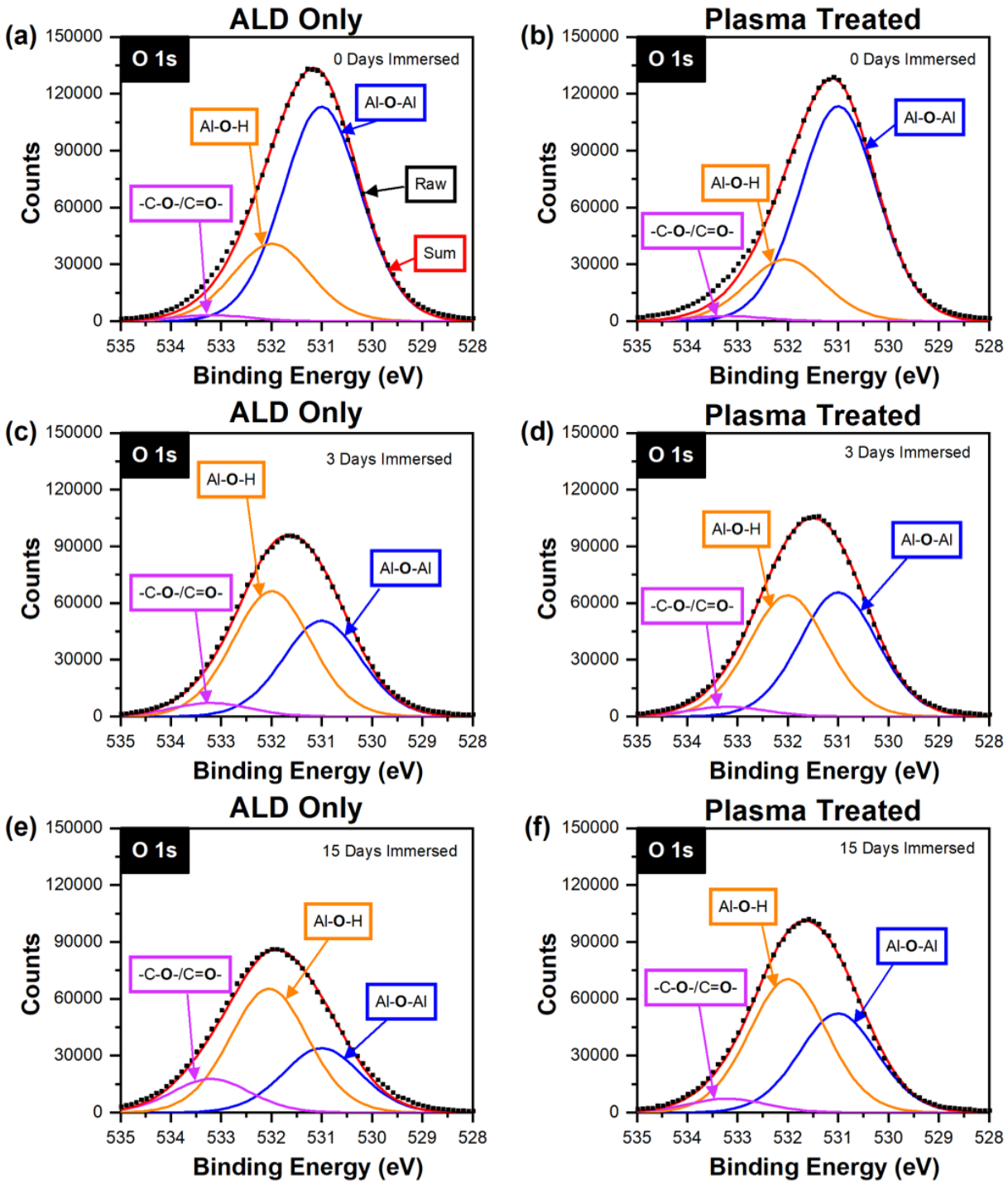

Figure 6: *Deconvoluted O 1s XPS spectra for ALD-only and plasma treated alumina films before and after water immersion. (a) ALD-only and (b) plasma-treated alumina freshly prepared. (c) ALD-only and (d) plasma-treated alumina after 3 days of immersion in 18 MOhm-cm DI water. (e) ALD-only and (f) plasma-treated alumina after 15 days of submersion in 18 MOhm-cm DI water.*

Individual deconvoluted peaks are labelled and colored by their assigned approximate binding environment. The summation of these deconvoluted peaks is plotted as a solid red line which can be compared to the raw data (black squares) in each plot as a measure of goodness of fit.

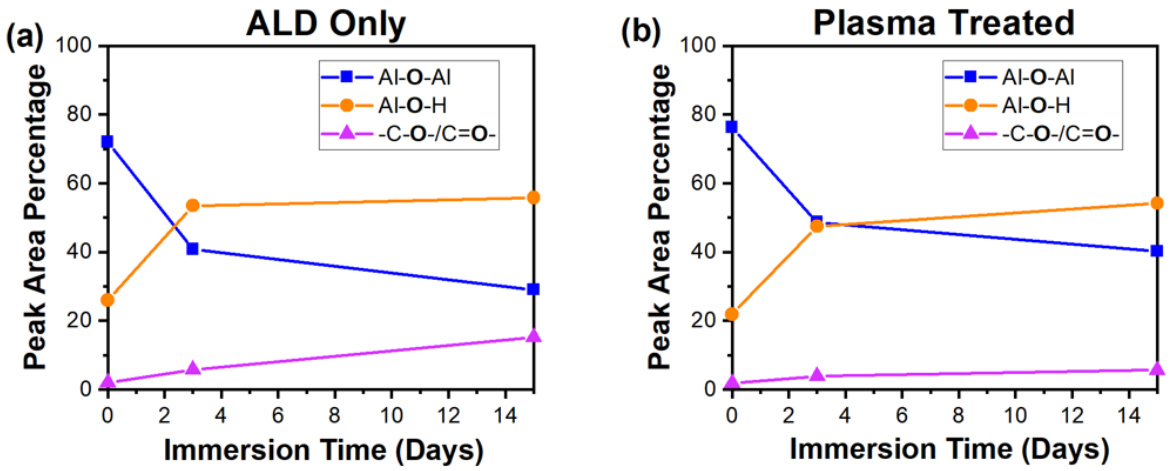

Figure 7: *Relative peak areas in the O 1s XPS spectra as a function of water immersion time for both (a) ALD-only and (b) plasma treated alumina films in 18 MOhm-cm DI water. Peak area percentages are calculated by dividing the peak area of the given peak by the combined area of all of the deconvoluted peaks for that O 1s spectrum. Data sets are labeled with their oxygen binding environments as assigned to the deconvoluted O 1s peaks.*

Deconvolution of the C 1s spectra can provide a possible explanation for the fourth peak at low binding energies appearing in both **Figures** 4 and 6. This deconvolution is given in the Supporting Information in figure S3. The C 1s spectra for the films are heavily influenced by air exposure time and environmental composition, as deposited adventitious carbon constitutes a large portion of the generated intensities. However, it is important to note that the adventitious carbon buildup measured here is a result of post-dissolution conditions, as all alumina films are subjected to dissolution in an identical timeframe post ALD-deposition. This feature is most evident in the fact that the zero-dissolution time (control) films for both plasma treated and ALD-only cases show lower signal-to-noise ratios of primary peaks and lower overall intensities due to their overall shorter synthesis-to-characterization air exposure times. Additionally, presence of a low energy

peak is confirmed for all films, suggesting that the identity of the low energy peak present in both the O 1s and Al 2p scans is some form of Al-**C**[38] complex resident from the ALD synthesis process, perhaps denoting residual partially reacted trimethyl aluminum structures incorporated directly into the films. The most notable change in the C 1s spectra with immersion time is the significant low energy shouldering of the C-**C**-O peak in the ALD-only films, which can be seen in figure S3. This overlap is shown as a new peak inserted adjacent to the fitted C-**C**-O (orange) peak that contains all the shouldering information when the position and the width of the C-**C**-O is held constant for each spectrum. This new peak is developed only for the ALD-only case at 9 days immersion (not shown) and is clearly visible and even surpasses the area of the C-**C**-O peak for the ALD-only films at 15 days immersion in water. The simultaneous generation of this peak with the formation of $Al(OH)_3$ as observed in Figure 4 is notable, and again suggests the presence of a restructured surface with increased hydroxylation, leading to a subtle shift in the chemical makeup of deposited hydrocarbons on the film surface evidenced by the low energy shouldering. This observation is a potential avenue for future studies involving intentional roughening of the alumina surface via water exposure to increase hydrocarbon adsorption rates.

To reinforce the supposition that the high energy (533.1 eV) peak observed in the O 1s spectra is in fact oxidized carbon, we compared the total integrated area of the four oxygen-containing peaks in the C 1s spectra to the area of the C-Ox peak in the O 1s spectra. The results are shown in figure S4. The total areas calculated from the two different elemental spectra roughly agree at all immersion times for both the plasma treated and ALD-only conditions independently, suggesting that the identity of the high energy peak in the O 1s spectra is in fact oxidized carbonaceous species of the types indicated in Figure 6.

Surprisingly, the ALD-only and plasma treated alumina films show very little difference in initial surface chemistry as demonstrated in the XPS spectra of **Figures** 4a and 4b and **Figures** 6a and 6b. These results suggest that a difference in surface chemistry cannot fully explain the subsequent difference in film hydration upon immersion and that the plasma treatment is perhaps causing more of a physical structural change than a chemical one. Thus, we hypothesize that the plasma treatment is inducing a localized densification of the amorphous ALD alumina. Densification of ceramic particles upon exposure to room temperature plasma is commonly used in nanoparticle synthesis, relying upon intense localized heating because of contact with the energized plasma.[20-22, 39] This localized densification could decrease the water permeability of the surface, reducing the rates of Reactions 1 and 2 to the point where complete film hydration and restructuring is not experienced within 15 days in aqueous DI solution.

4.3 Dissolution of ALD-only and Plasma Treated Alumina Thin Films in Other Aqueous Solutions: To provide a broader understanding of ALD alumina's aqueous degradation behavior, we further studied the degrdation of both ALD-only and plasma treated alumina films in aqueous solutions of varying pH, ionicity, and reaction chemistry. **Figure** 8 summarizes these results. In the ALD-only case (**Figure** 8a), alumina films are unstable in all measured solutions, including solutions with basic (pH = 13.0) acidic (pH = 1.0) and neutral (water and salt) pH values. However, alumina films receiving a post-deposition air plasma anneal exhibit stability in neutral pH solutions for up to 25 days, including water solutions of various purities and salt concentrations (**Figure** 8b). However, these plasma treated alumina films show no improvement in stability in acidic or basic solutions, consistent with thermodynamic expectations. Interestingly, the plasma treated alumina is also unstable in the PBS buffer solution (pH = 7.0).

The difference in dissolution rates for acidic and basic conditions does not vary significantly between the ALD-only and plasma treated conditions. This similarity in acidic and basic dissolution behavior further suggests that the difference between ALD-only and plasma treated alumina films is not a chemical difference but rather a physical structure difference.

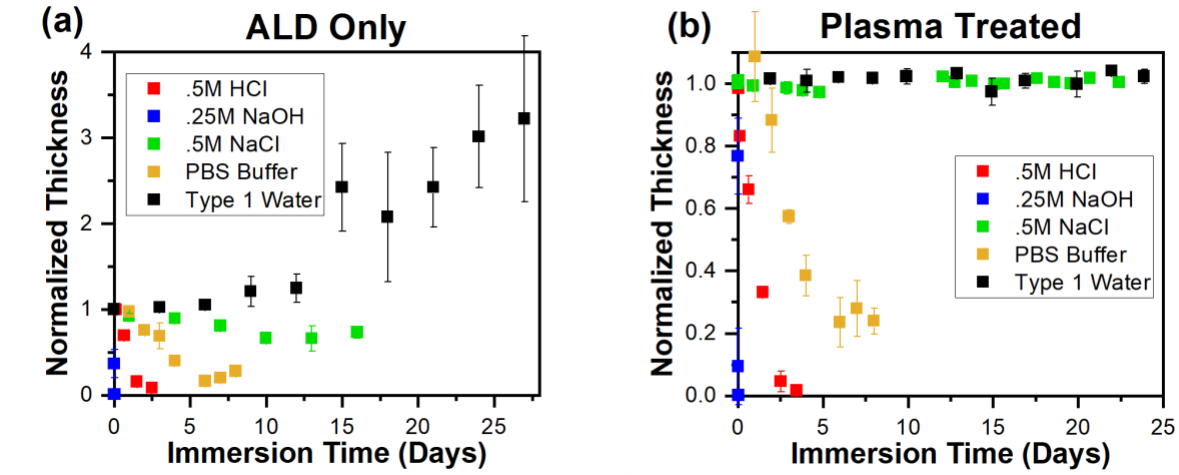

Figure 8: *Temporal plots of alumina dissolution in various aqueous solutions for (a) ALD-only and (b) plasma treated alumina thin films. Film thickness was measured with ex situ ellipsometry and normalized to the initial film thickness. Buffer solution is a pH 7 PBS. Type I water is DI water purchased directly from Sigma Aldrich. Note that ordinate axes have different scales in panel (a) and (b).*

Interestingly, the ALD-only alumina films exhibit different instability behaviors in neutral pH values depending upon ionic concentration. This behavior is exemplified by the Type I water data set (black squares) and 0.5 M NaCl aqueous solution (green squares) data sets in Figure 8a. The ALD-only alumina films grow thicker or hydrate in the deionized Type I water while film dissolution is observed in the 0.5 M NaCl water. This result suggests that solution ions play a role in altering dissolution of hydrated alumina species and is consistent with prior observations made by Correa *et al.*[12] This phenomenon warrants further investigation to determine the onset of

dissolution and the exact chemistry of the dissolved species. In contrast, the plasma treated alumina films remain completely stable in neutral pH aqueous solutions irrespective of ion content.

Figure 9 summarizes the general stability / instability behavior found in this study for amorphous ALD alumina thin films without and with a post-deposition air plasma anneal in various aqueous solutions of widely ranging "corrosiveness".

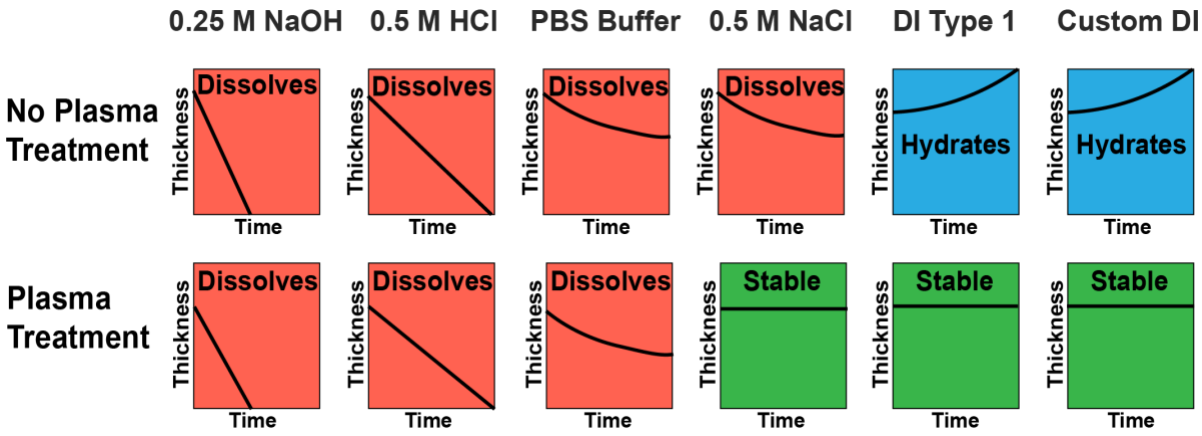

Figure 9: *Summary of amorphous ALD alumina film stability over a range of aqueous solution conditions without and with a post-deposition air plasma anneal. Individual boxes are color coded corresponding to their approximate stability: green = stable; red = dissolves; blue = hydrates. Line slopes are approximations of behavior based on collected ellipsometry data.*

Conclusion

The aqueous stability of ALD synthesized amorphous alumina thin films was re-examined. XPS investigations revealed that the metastable amorphous alumina phase typically formed with low-temperature (< 200 °C) ALD processing is susceptible to hydration and/or dissolution in near neutral (pH = 7) aqueous conditions, counter to what is expected for the crystalline phase. The as-deposited alumina films are found to contain oxide and oxyhydroxide (AlOOH) species as well as

some adsorbed water. When immersed in deionized water, more oxyhydroxide species form. These oxyhydroxides eventually convert to hydroxides ($Al(OH)_3$), leading to an observable increase in film thickness. ALD alumina films immersed in near neutral aqueous solutions of high ionic content (high salt concentrations) are also found to dissolve.

In contrast, brief post-deposition exposures of ALD alumina films to an air plasma anneal imparts significant stability to the film in aqueous environments. These plasma annealed ALD alumina films exhibit no change in film thickness after 30 days of immersion in deionized or high ionic content water of pH = 7. While XPS analysis reveals little difference in the initial chemical structure of the plasma treated alumina films, much less hydration is observed in XPS analysis of water immersed plasma treated alumina films. XPS analysis reveals that after 15 days of immersion in DI water for the plasma-exposed films, no $Al(OH)_3$ are detected and only about a quarter of the near-surface aluminum atoms are in an oxyhydroxide oxidation state, likely attributable to true surface hydroxyls. However, this stability does not extend to extreme pH values where even fully crystalline alumina is thermodynamically expected to dissolve, suggesting that the plasma treatment is creating more of a physical change in the structure (i.e., densifying the near surface) rather than a chemical change. The simplicity and effectiveness of this plasma treatment can provide a low-temperature alternative to high-temperature (>700 °C) thermal annealing to impart the chemical stability often desired for ALD alumina barrier layers.

Supporting Information. Survey of XPS results, reproducibility and error analysis of ellipsometry measurements, full C1s XPS deconvolution, integrated C-Ox counts for both O1s and C1s deconvolutions

Acknowledgements:

This research was partially supported by an Early-Career Research Fellowship from the Gulf Research Program of the National Academies of Sciences, Engineering, and Medicine (Grant # 2000009646) and by the National Science Foundation CHE CAT program under Grant No. 1954809. This work was performed in part at the Georgia Tech Institute for Electronics and Nanotechnology, a member of the National Nanotechnology Coordinated Infrastructure (NNCI), which is supported by the National Science Foundation (ECCS-2025462). E.K.M. was supported by the Department of Defense (DoD) through the National Defense Science and Engineering Graduate (NDSEG) Fellowship Program. Y. Li was supported by a fellowship from the Renewable Bioproducts Institute at Georgia Tech.

References

1. Kim, L. H.; Kim, K.; Park, S.; Jeong, Y. J.; Kim, H.; Chung, D. S.; Kim, S. H.; Park, C. E., Al2O3/TiO2 Nanolaminate Thin Film Encapsulation for Organic Thin Film Transistors via Plasma-Enhanced Atomic Layer Deposition. *ACS Applied Materials & Interfaces* **2014,** *6* (9), 6731-6738.
2. Dameron, A. A.; Davidson, S. D.; Burton, B. B.; Carcia, P. F.; McLean, R. S.; George, S. M., Gas Diffusion Barriers on Polymers Using Multilayers Fabricated by Al2O3 and Rapid SiO2 Atomic Layer Deposition. *The Journal of Physical Chemistry C* **2008,** *112* (12), 4573-4580.
3. Wang, C.-Y.; Fuentes-Hernandez, C.; Yun, M.; Singh, A.; Dindar, A.; Choi, S.; Graham, S.; Kippelen, B., Organic Field-Effect Transistors with a Bilayer Gate Dielectric Comprising an Oxide Nanolaminate Grown by Atomic Layer Deposition. *ACS Applied Materials & Interfaces* **2016,** *8* (44), 29872-29876.
4. Marin, E.; Guzman, L.; Lanzutti, A.; Ensinger, W.; Fedrizzi, L., Multilayer Al2O3/TiO2 Atomic Layer Deposition coatings for the corrosion protection of stainless steel. *Thin Solid Films* **2012,** *522*, 283-288.
5. Finch, D. S.; Oreskovic, T.; Ramadurai, K.; Herrmann, C. F.; George, S. M.; Mahajan, R. L., Biocompatibility of atomic layer-deposited alumina thin films. *Journal of Biomedical Materials Research Part A* **2008,** *87A* (1), 100-106.
6. George, C.; Littlewood, P.; Stair, P. C., Understanding Pore Formation in ALD Alumina Overcoats. *ACS Applied Materials & Interfaces* **2020,** *12* (18), 20331-20343.
7. Bulusu, A.; Singh, A.; Wang, C. Y.; Dindar, A.; Fuentes-Hernandez, C.; Kim, H.; Cullen, D.; Kippelen, B.; Graham, S., Engineering the mechanical properties of ultrabarrier films grown by atomic layer deposition for the encapsulation of printed electronics. *Journal of Applied Physics* **2015,** *118* (8), 085501.
8. Marquardt, A. E.; Breitung, E. M.; Drayman-Weisser, T.; Gates, G.; Phaneuf, R. J., Protecting silver cultural heritage objects with atomic layer deposited corrosion barriers. *Heritage Science* **2015,** *3* (1), 37.
9. George, S. M., Atomic Layer Deposition: An Overview. *Chemical Reviews* **2010,** *110* (1), 111-131.
10. Parsons, G. N.; George, S. M.; Knez, M., Progress and future directions for atomic layer deposition and ALD-based chemistry. *MRS Bulletin* **2011,** *36* (11), 865-871.
11. Puurunen, R. L., Surface chemistry of atomic layer deposition: A case study for the trimethylaluminum/water process. *Journal of Applied Physics* **2005,** *97* (12), 121301.
12. Correa, G. C.; Bao, B.; Strandwitz, N. C., Chemical Stability of Titania and Alumina Thin Films Formed by Atomic Layer Deposition. *ACS Applied Materials & Interfaces* **2015,** *7* (27), 14816-14821.
13. Deltombe, E.; Vanleugenhaghe, C.; Pourbaix, M. Aluminium. In *Atlas of Electrochemical Equilibria in Aqueous Solutions*, Vol. 2; National Association of Corrosion Engineers, 1974; pp 168-175.
14. Fan, R.; Dong, W.; Fang, L.; Zheng, F.; Su, X.; Zou, S.; Huang, J.; Wang, X.; Shen, M., Stable and efficient multi-crystalline n+p silicon photocathode for H2 production with pyramid-like surface nanostructure and thin Al2O3 protective layer. *Applied Physics Letters* **2015,** *106* (1), 013902.
15. Bulusu, A.; Kim, H.; Samet, D.; Graham, S., Improving the stability of atomic layer deposited alumina films in aqueous environments with metal oxide capping layers. *Journal of Physics D-Applied Physics* **2013,** *46* (8).
16. Abdulagatov, A. I.; Yan, Y.; Cooper, J. R.; Zhang, Y.; Gibbs, Z. M.; Cavanagh, A. S.; Yang, R. G.; Lee, Y. C.; George, S. M., Al2O3 and TiO2 Atomic Layer Deposition on Copper for Water Corrosion Resistance. *ACS Applied Materials & Interfaces* **2011,** *3* (12), 4593-4601.
17. Adiga, S. P.; Zapol, P.; Curtiss, L. A., Structure and Morphology of Hydroxylated Amorphous Alumina Surfaces. *The Journal of Physical Chemistry C* **2007,** *111* (20), 7422-7429.

18. Zhang, Y.; Zhang, Y.-Z.; Miller, D. C.; Bertrand, J. A.; Jen, S.-H.; Yang, R.; Dunn, M. L.; George, S. M.; Lee, Y. C., Fluorescent tags to visualize defects in Al2O3 thin films grown using atomic layer deposition. *Thin Solid Films* **2009,** *517* (24), 6794-6797.
19. Gorham, C. S.; Gaskins, J. T.; Parsons, G. N.; Losego, M. D.; Hopkins, P. E., Density dependence of the room temperature thermal conductivity of atomic layer deposition-grown amorphous alumina (Al2O3). *Applied Physics Letters* **2014,** *104* (25), 253107.
20. Bapat, A.; Anderson, C.; Perrey, C. R.; Carter, C. B.; Campbell, S. A.; Kortshagen, U., Plasma synthesis of single-crystal silicon nanoparticles for novel electronic device applications. *Plasma Physics and Controlled Fusion* **2004,** *46* (12B), B97-B109.
21. Mangolini, L.; Kortshagen, U., Selective nanoparticle heating: Another form of nonequilibrium in dusty plasmas. *Physical Review E* **2009,** *79* (2), 026405.
22. Szalay, Z.; Bodišová, K.; Pálková, H.; Švančárek, P.; Dˇurina, P.; Ráhelˇ, J.; Zahoranová, A.; Galusek, D., Atmospheric pressure air plasma treated alumina powder for ceramic sintering. *Ceramics International* **2014,** *40* (8, Part B), 12737-12743.
23. Piercy, B. D.; Losego, M. D., Tree-based control software for multilevel sequencing in thin film deposition applications. *Journal of Vacuum Science & Technology B* **2015,** *33* (4), 043201.
24. Barin, I.; Sauert, F. Ag-$AuTe_2$. In *Thermochemical Data of Pure Substances*, 3rd ed.; VCH, 1989; pp 1-103.
25. Chase, M. W. J. Aluminum. In *NIST-JANAF Thermochemical Tables*, 4th ed.; American Inst. of Physics, 1998; pp 150-159.
26. Kloprogge, J. T.; Duong, L. V.; Wood, B. J.; Frost, R. L., XPS study of the major minerals in bauxite: Gibbsite, bayerite and (pseudo-)boehmite. *Journal of Colloid and Interface Science* **2006,** *296* (2), 572-576.
27. Ben Amor, S.; Baud, G.; Jacquet, M.; Nansé, G.; Fioux, P.; Nardin, M., XPS characterisation of plasma-treated and alumina-coated PMMA. *Applied Surface Science* **2000,** *153* (2), 172-183.
28. Iatsunskyi, I.; Kempiński, M.; Jancelewicz, M.; Załęski, K.; Jurga, S.; Smyntyna, V., Structural and XPS characterization of ALD Al2O3 coated porous silicon. *Vacuum* **2015,** *113*, 52-58.
29. Lefèvre, G.; Duc, M.; Lepeut, P.; Caplain, R.; Fédoroff, M., Hydration of γ-Alumina in Water and Its Effects on Surface Reactivity. *Langmuir* **2002,** *18* (20), 7530-7537.
30. He, H.; Alberti, K.; Barr, T. L.; Klinowski, J., ESCA studies of aluminophosphate molecular sieves. *The Journal of Physical Chemistry* **1993,** *97* (51), 13703-13707.
31. Alexander, M. R.; Thompson, G. E.; Beamson, G., Characterization of the oxide/hydroxide surface of aluminium using x-ray photoelectron spectroscopy: a procedure for curve fitting the O 1s core level. *Surface and Interface Analysis* **2000,** *29* (7), 468-477.
32. Malki, A.; Mekhalif, Z.; Detriche, S.; Fonder, G.; Boumaza, A.; Djelloul, A., Calcination products of gibbsite studied by X-ray diffraction, XPS and solid-state NMR. *Journal of Solid State Chemistry* **2014,** *215*, 8-15.
33. van den Brand, J.; Snijders, P. C.; Sloof, W. G.; Terryn, H.; de Wit, J. H. W., Acid−Base Characterization of Aluminum Oxide Surfaces with XPS. *The Journal of Physical Chemistry B* **2004,** *108* (19), 6017-6024.
34. Konstadinidis, K.; Thakkar, B.; Chakraborty, A.; Potts, L. W.; Tannenbaum, R.; Tirrell, M.; Evans, J. F., Segment level chemistry and chain conformation in the reactive adsorption of poly(methyl methacrylate) on aluminum oxide surfaces. *Langmuir* **1992,** *8* (5), 1307-1317.
35. Ealet, B.; Elyakhloufi, M. H.; Gillet, E.; Ricci, M., Electronic and crystallographic structure of γ-alumina thin films. *Thin Solid Films* **1994,** *250* (1), 92-100.
36. Olefjord, I.; Nylund, A., Surface analysis of oxidized aluminium. 2. Oxidation of aluminium in dry and humid atmosphere studied by ESCA, SEM, SAM and EDX. *Surface and Interface Analysis* **1994,** *21* (5), 290-297.

37. Wu, Y.; Mayer, J. T.; Garfunkel, E.; Madey, T. E., X-ray Photoelectron Spectroscopy Study of Water Adsorption on BaF2(111) and CaF2(111) Surfaces. *Langmuir* **1994,** *10* (5), 1482-1487.
38. Bou, M.; Martin, J. M.; Le Mogne, T.; Vovelle, L., Chemistry of the interface between aluminium and polyethyleneterephthalate by XPS. *Applied Surface Science* **1991,** *47* (2), 149-161.
39. Maurer, H. R.; Kersten, H., On the heating of nano- and microparticles in process plasmas. *Journal of Physics D: Applied Physics* **2011,** *44* (17), 174029.

TOC Graphic

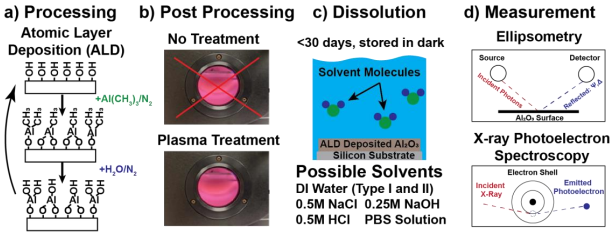
a) Processing
Atomic Layer Deposition (ALD)
+Al(CH3)3/N2
+H2O/N2
b) Post Processing
No Treatment
Plasma Treatment
c) Dissolution
<30 days, stored in dark
Solvent Molecules
ALD Deposited Al2O3
Silicon Substrate
Possible Solvents
DI Water (Type I and II)
0.5M NaCl 0.25M NaOH
0.5M HCl PBS Solution
d) Measurement
Ellipsometry
Source
Detector
Incident Photons
Reflected Light
Al2O3 Surface
X-ray Photoelectron Spectroscopy
Electron Shell
Incident X-Ray
Emitted Photoelectron